

Development of hazard map for deep-seated landslide using stochastic response surface method

Kiyonobu Kasama¹ and H. Tanaka²

¹ Graduate School of Kyushu University, 744 Motoooka, Nishi-ku, Fukuoka 819-0395, Japan.

² Obayashi Corporation Co., Ltd., 2-15-2 Kounan, Minato-ku, Tokyo 108-8502, Japan.

ABSTRACT

This paper presents a numerical procedure to develop a hazard map for a deep-seated landslide using the stochastic response surface method considering the uncertainty of strength parameters. The following conclusions are drawn from this study; (1) Based on the parametric study of 3D slope stability analysis, the cohesion of 110kPa and the frictional angle of 35° are estimated for the deep-seated landslide at Tateno area in Kumamoto prefecture caused by the 2016 Kumamoto earthquake, Japan. (2) The failure probability of seep-seated landslide for the foreshock and main shock of the 2016 Kumamoto earthquake are estimated to be 30% and almost 100% respectively. (3) Under the situation having the uncertainty of material parameters, the stochastic response surface method using the polynomial chaos expansion is useful for developing a hazard map for the failure probability and the arrival risk of a large-scale landslide such as a deep-seated landslide.

Keywords: deep-seated landslide; hazard map; reliability; probability; stochastic response surface method

1 INTRODUCTION

The number of a large-scale slope failure, called deep-seated landslide, has increased due to torrential rainfall induced by climate change and megathrust earthquake induced by recent active tectonic movement. A conventional hardware countermeasure such as ground anchor is not effective for deep-seated landslide because the size and area of countermeasure should be very large and wide. Therefore, software countermeasure such as hazard map and evacuation alert is useful for deep-seated landslide. However, the soil profile such as material property and strength parameter around natural slope is not well investigated and also contains spatial variability and uncertainty for the estimation. From these back ground, this paper presents a numerical procedure to develop a hazard map for a deep-seated landslide using the stochastic response surface method considering the uncertainty of strength parameters.

2 DEEP-SEATED LANDSLIDE IN JAPAN

The target landslide for this study is a deep-seated landslide at Tateno area in Kumamoto prefecture in Japan caused by the main shock of the 2016 Kumamoto earthquake (Mukunoki et al. 2018). The length and width are 750 m and 200 m respectively while the volume of collapsed rocks and soils due to the landslide is about 50K m³. The collapsed rocks and soils had interrupted the national road No. 57 and Japan railway

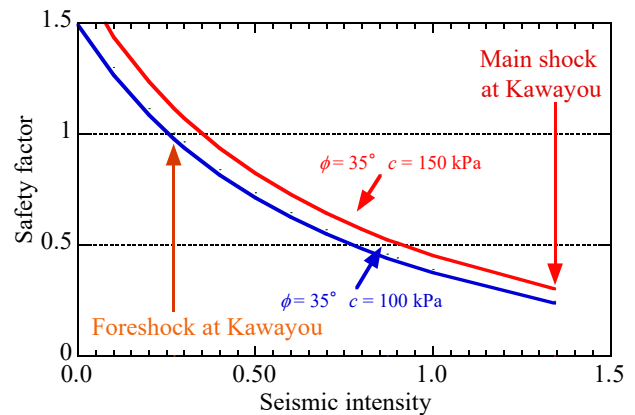


Fig. 1. Safety factor and seismic intensity.

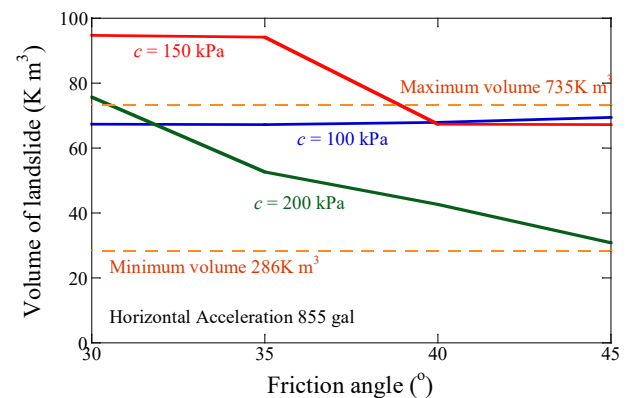
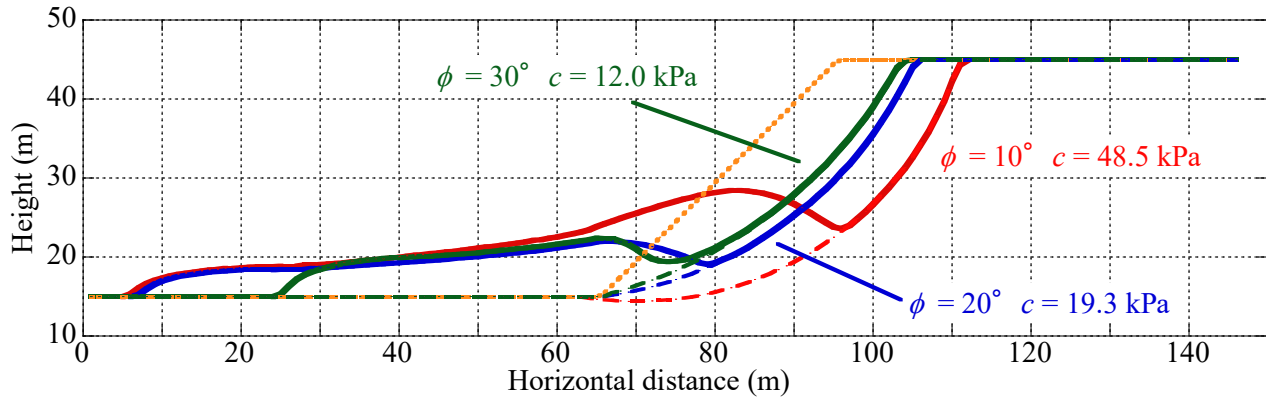
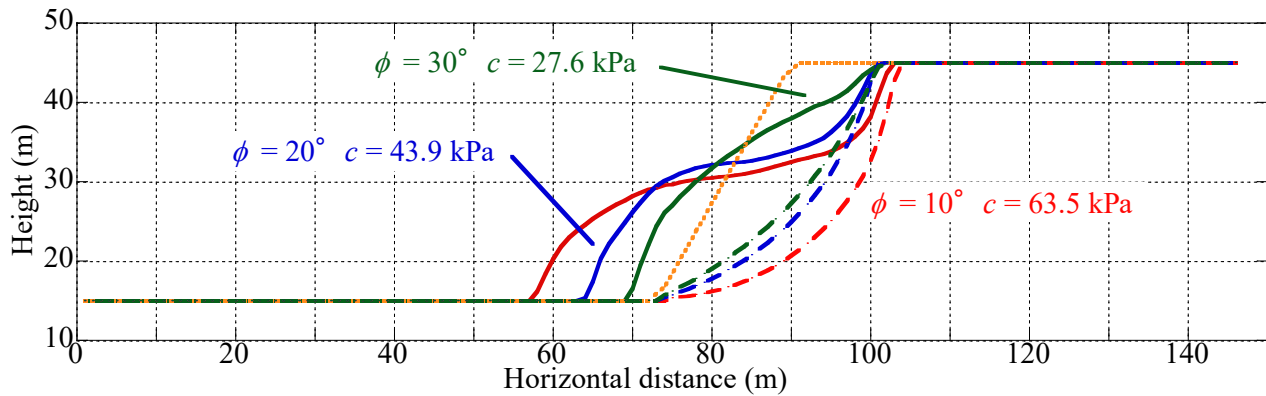


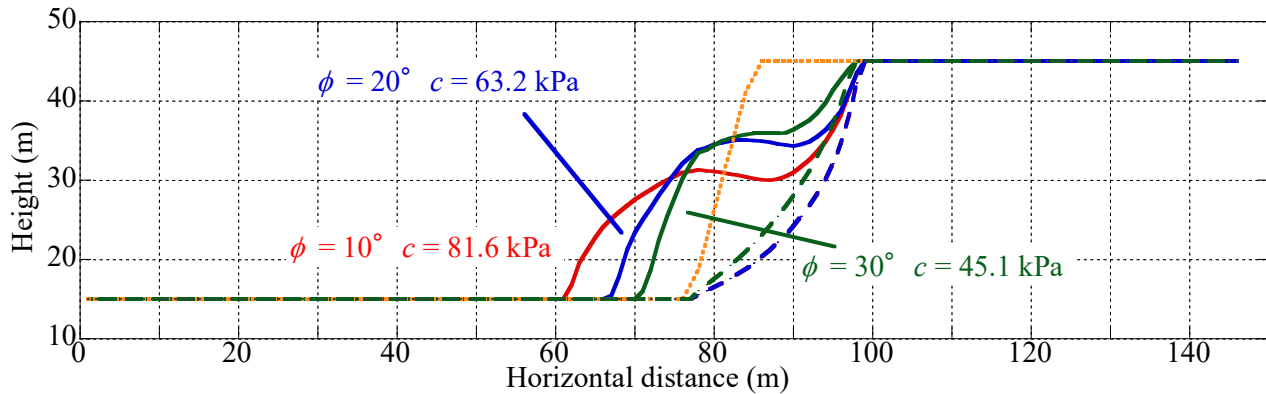
Fig. 2. The volume of collapsed rocks and soils. for more than three months.



a) $\theta = 45^\circ$



b) $\theta = 60^\circ$



c) $\theta = 75^\circ$

Fig. 3. The numerical result of runout analysis for a given slope angle.

In order to estimate the cohesion and friction angle of slope, three dimensional slope stability analysis was carried out. It is assumed that the unit soil weight is 23.0 kN/m^3 from geological survey and there is no ground water in slope. It can be emphasized that optimum cohesion and friction angel are determined from the viewpoints of matching of the collapsed area of deep-seated landslide, the occurrence of landslide by the seismic intensity corresponded to the main shock of the 2016 Kumamoto Earthquakes and the volume of landslide.

Fig. 1 shows the estimated safety factor from 3D slope stability analysis (Reid et al. 2015) against horizontal seismic acceleration. It is noted that magnitudes of foreshock and main shock of the 2016 Kumamoto earthquakes at the closest observation point, Kawayou, are shown in this figure. Estimated safety factor decreases with increasing horizontal seismic intensity. In order to satisfy the condition that the safety factor is less than 1.0 at the main shock while the safety factor is more than 1.0 at foreshock, the cohesion more than 100kPa and friction angle of 35° are obtained.

Fig. 2 shows the volume of landslide obtained by the result of parametric study of 3D slope stability analysis. The actual volume of deep-seated landslide by survey is estimated to range from 280K m³ to 730K m³. The volume seems to decrease with increasing cohesion and friction angle. In addition, it can be seen that numerical results for cohesion from 50kPa to 150kPa match the actual failure location while that for cohesion of 200kPa is away from the actual failure location. From these examinations, the cohesion and friction angle are estimated to be 110kPa and 35° respectively for the target deep-seated landslide.

3 STOCHASTIC RESPONSE SURFACE METHOD

3.1 Runout analysis of collapsed landslide

After identifying the collapsed landslide area by the 3D slope stability analysis, the runout analysis of collapsed landslide is carried out. The runout analysis uses a continuum model to simulate the behavior of collapsed landslide. In the runout analysis of this study, it is characterized that collapsed landslide is divided into vertical soil columns and active and passive earth pressures from surrounding soil columns is considered as a driving force depending on the volume change of soil column in addition to the self-weight of column.

Fig. 3 shows numerical results of the runout analysis of collapsed landslide for a 2D model slope with the slope angle of 45°, 60° and 75° and the height of 30m. It is seen that travel distance of collapsed soils increases with decreasing cohesion and friction angle and increasing slope angle. It can be characterized that the travel distance is within the height from the toe of slope when the slope angle is more than 60°.

3.2 Stochastic response surface method

The risk of deep-seated landslide is evaluated by the stochastic response surface method using the polynomial expansion (Isukapalli et al. 1998 and). In the polynomial chaos expansion, an objective function is expressed by the polynomial of normal random numbers and the statistical values such as mean and standard deviation can be estimated by the limited number of outputs. In this study, uncertain input parameters X_i such as cohesion and friction angle are assumed to be modeled as a normal distribution with mean μ_i and standard deviation σ_i and normal random number ξ as follows.

$$X_i = \mu_i + \sigma_i \cdot \xi \quad (1)$$

The objective function f^* is approximated by the polynomial of normal random number as follows.

Coefficient of variation, COV of c	0.1, 0.2, 0.3
Friction angle ϕ	35°
Coefficient of variation, COV of ϕ	0.1, 0.2, 0.3
Unit soil weight γ	23.0 kN/m ³
Seismic intensity k_h	0, 0.2, 0.843, 1.34 (g)

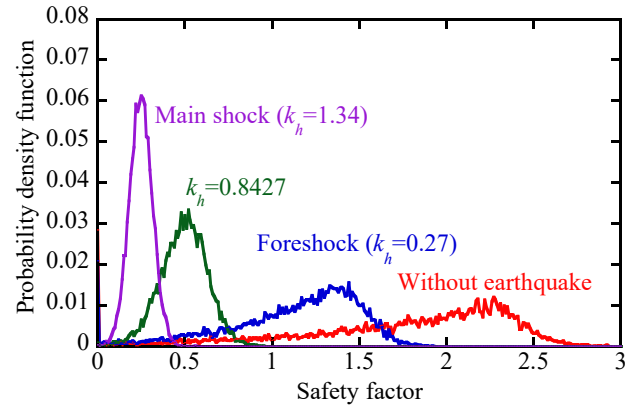


Fig. 4. PFD of safety factor for a given seismic intensity.

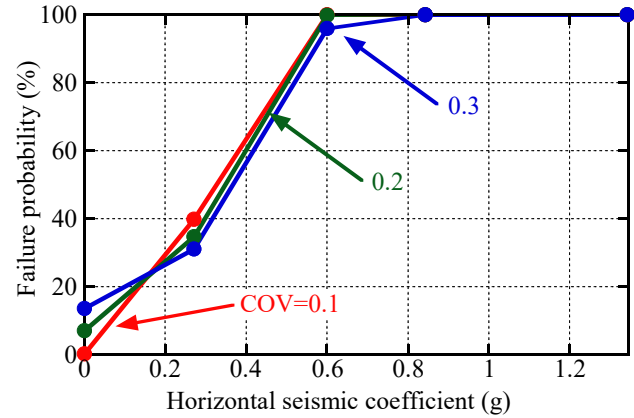


Fig. 5. Failure probability against seismic intensity.

$$f^* = \sum_{j=0}^P f_j \cdot \Psi_j(\xi) \quad (2)$$

where f_j is the coefficient of polynomial, Ψ is the orthogonal basis function of normal random number ξ , P is the number of polynomial function. It is noted that P is 6 because second-order polynomial used in this study. In addition, the safety factor and thickness of deep-seated landslide was selected as the objective function. Mean and standard deviation of the objective function are estimated by the following equation.

$$\mu_{f^*} = E[f^*(\xi)] = f_0 \quad (3)$$

$$\sigma_{f^*}^2 = \sum_{j=1}^P f_j^2 \cdot \langle \Psi_j^2(\xi) \rangle \quad (4)$$

Table 1. Estimated strength parameter

Cohesion c	110 kPa
--------------	---------

Table 1 shows input parameter in this study. Mean value of cohesion and friction angle was determined by back analysis shown in prior section. The coefficient of variation of c and ϕ is assumed as 0.1, 0.2 and 0.3. The horizontal seismic intensity was assumed as 0 (normal condition without earthquake), 0.27 (the seismic intensity of the foreshock at Kawayou), 0.84 (the main shock observed at Nakamatsu) and 1.34 (the main shock at Kawayou).

3.3 Failure probability and arrival risk

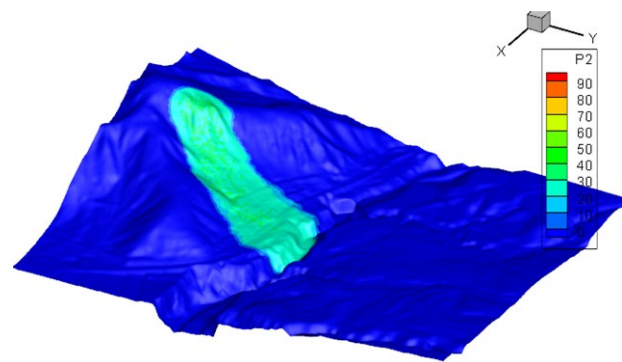
Fig. 4 shows the probability distribution function, PDF, of the safety factor obtained by the proposed stochastic response surface method for a given seismic intensity. It is seen that mean safety factor decreases with increasing seismic intensity while the range of PDF decreases with increasing seismic intensity. Moreover, polynomial chaos expansion using Equation in this study can flexibly express the PDF depending the seismic intensity.

Fig. 5 shows the relationship between the failure probability of deep-seated landslide and horizontal seismic intensity for a given the coefficient of variation. The failure probability of landslide lineally increases with increasing seismic intensity irrespective of COV 's of strength parameters. Failure probabilities under normal condition (without earthquake) are 0.31 % for $COV = 0.1$ and 13.6 % for $COV = 0.3$. The failure probability for the foreshock is estimated to be from 30 % to 40 % while the failure probability for the main shock is estimated to be more than 99%. Therefore, the risk of landslide by the main shock is comparably high irrespective of the spatial variability and uncertainty of strength parameters.

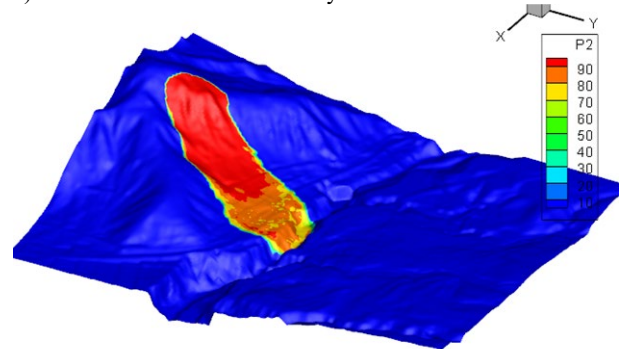
In order to estimate an arrival risk for the runout of deep-seated landslide, the thickness of landslide obtained by the runout analysis is selected as an objective function. Fig. 6 shows the arrival risk of deep-seated landslide for foreshock and main shock of the 2016 Kumamoto earthquakes. It is noted that the arrival risk means the probability that the cover thickness of rocks and soils deposited by collapsed landslide is estimated more than 1.0 m. The arrival risk due to the foreshock for the national road No. 57 and Hohi Japan railway is estimated to be 30 % while that for the main shock is estimated to be over 80 % indicating there is a high risk for infrastructure such as road and railway.

4 CONCLUSION

This paper presents a numerical procedure to develop a hazard map for a deep-seated landslide using the stochastic response surface method considering the uncertainty of strength parameters. The following conclusions are drawn from this study; (1) Based on the parametric study of 3D slope stability analysis, the cohesion of 110kPa and the frictional angle of 35° are estimated for the deep-seated landslide at Tateno area



a) Foreshock for seismic intensity = 0.27.



b) Main shock for seismic intensity = 1.34.

Fig. 6. Arrival risk of collapsed rocks and soils more than 1.0 m.

in Kumamoto prefecture caused by the 2016 Kumamoto earthquake, Japan. (2) The failure probability of seep-seated landslide for the foreshock and main shock of the 2016 Kumamoto earthquake are estimated to be 30% and almost 100% respectively. (3) Under the situation having the uncertainty of material parameters, the stochastic response surface method using the polynomial chaos expansion is useful for developing a hazard map for the failure probability and the arrival risk of a large-scale landslide such as a deep-seated landslide.

REFERENCES

- Isukapalli, S. S., Roy, A. and Georgopoulos, P. G. (1998). Stochastic Response Surface Methods (SRSMs) for Uncertainty Propagation: Application to Environmental and Biological Systems, Risk Analysis, Vol. 18, No. 3, pp. 351-363.
- Li, D. Q., Zheng, D., Cao, Z. J., Tang, X. S. and Phoon, K. K. (2016). Response surface methods for slope reliability analysis: Review and comparison, Engineering Geology, Vol. 203, pp. 3-14.
- Mukunoki, T., Kasama, K., Murakami, S., Ikemi, H., Ishikura, R., Fujikawa, T., Yasufuku, N. and Kitazono, T. (2016). Reconnaissance report on geotechnical damage caused by an earthquake with JMA seismic intensity 7 twice in 28 h, Kumamoto, Japan, Soils and Foundations, Vol.56, No.6, pp. 947-964.
- Reid, M. E. Christian, S. B, Brien, D. L, and Henderson, S. T. (2015). Scoops3D-Software to analyze three-dimensional slope stability throughout a digital landscape: U.S Geological Survey Techniques and Methods, Chapter-2. Basis of the Slope-Stability Analysis, pp.7-26.